Structural replacements for the benzoxazinone protox inhibitors†

John W Lyga,* Jun H Chang, George Theodoridis and Jonathan S Baum

Discovery Research Department, Agricultural Products Group, FMC Corporation, PO Box 8, Princeton, New Jersey 08543, USA

Abstract: Substituted benzoxazinones are a class of highly active inhibitors of protoporphyrinogen oxidase (protox) which are effective at controlling grass and broadleaf weeds at low rates. As part of the process of optimization of the herbicidal activity of the 6-heterocyclic benzoxazinones, a number of replacements were prepared for the oxazinone ring. Quantitative structure–activity relationships (QSAR) were developed for the benzoxazinone replacements using molecular properties, and these were compared to published QSAR for the acyclic 2,4,5-trisubstituted arylheterocyclic protox inhibitors. That the molecular properties of the acyclic and bicyclic protox inhibitors are similar suggest they may be interacting with the same binding site.

Keywords: benzoxazinone; protox inhibitor; herbicide; QSAR

1 INTRODUCTION

The tetrahydrophthalimide benzoxazinone class of herbicides (Fig 1; **1**) were first reported in the mid 1980s by Sumitomo Chemical Company.[1] Our own work in this area led to the discovery of several other highly active substituted heterocyclic benzoxazinones, including the 1,2,4-triazolin-5-ones (**2**), 1,2,4-triazine-3,5-diones (**3**) and the 1,2,3,4-tetrazolin-5-ones (**4**).[2–4] Substituted benzoxazinones are a class of highly active inhibitors of protoporphyrinogen oxidase (protox) which are effective at controlling grass and broadleaf weeds at low rates (Fig 1).

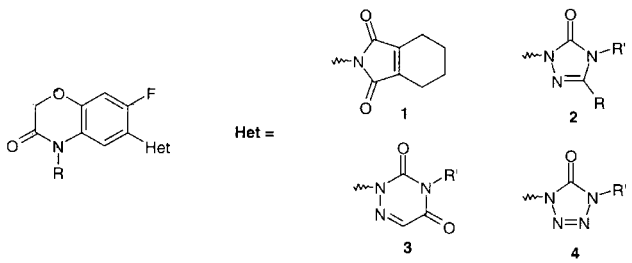

Het R=C_3H_7	R′	Velvetleaf pre-emergence ED_{85} (g ha^{-1})	Johnsongrass pre-emergence ED_{85} (g ha^{-1})
1		62	250
2	CF_2H	15	32
3	CH_3	32	32
4	$CH_2CH_2CH_2F$	63	125

Figure 1. Structure and herbicidal activity of the benzoxazinone herbicides.

One of the reasons we became interested in the bicyclic protox inhibitors was the differences in structure–activity relationships between the acyclic and bicyclic compounds. Our published QSAR for the acyclic 2,4,5-trisubstituted arylheterocyclic protox inhibitors indicate that the greatest activity is observed for compounds having small, hydrophobic, electronegative groups at position **4**; steric considerations seem to be important at position 5.[5–8] The benzoxazinone SAR does not seem to fit these rules. For example, the acyclic isostere (**5**) was over 30-fold less active against broadleaf weeds than the benzoxazinone (**6**) (Fig 2). To better understand whether the bicyclic herbicides interact with protox in a different manner from the acyclics, we proceeded to develop a QSAR model for the former. A preliminary report of this work was given at a recent American Chemical Society Conference.[9]

2 MATERIALS AND METHODS

2.1 Chemicals

General synthetic methods for the test compounds are outlined in Figs 3–8. Detailed syntheses of the

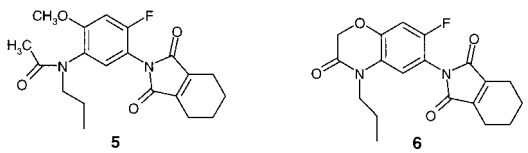

Figure 2. Structures for compounds **5** and **6**.

* Correspondence to: John W Lyga, Discovery Research Department, Agricultural Products Group, FMC Corporation, PO Box 8, Princeton, NJ 08543, USA.
† Based on poster presentations at the 9th International Congress of Pesticide Chemistry, organised by the International Union of Pure and Applied Chemistry (IUPAC), and held in London, UK, 2–7 August 1998.
(*Received 6 October 1998; accepted 23 November 1998*)

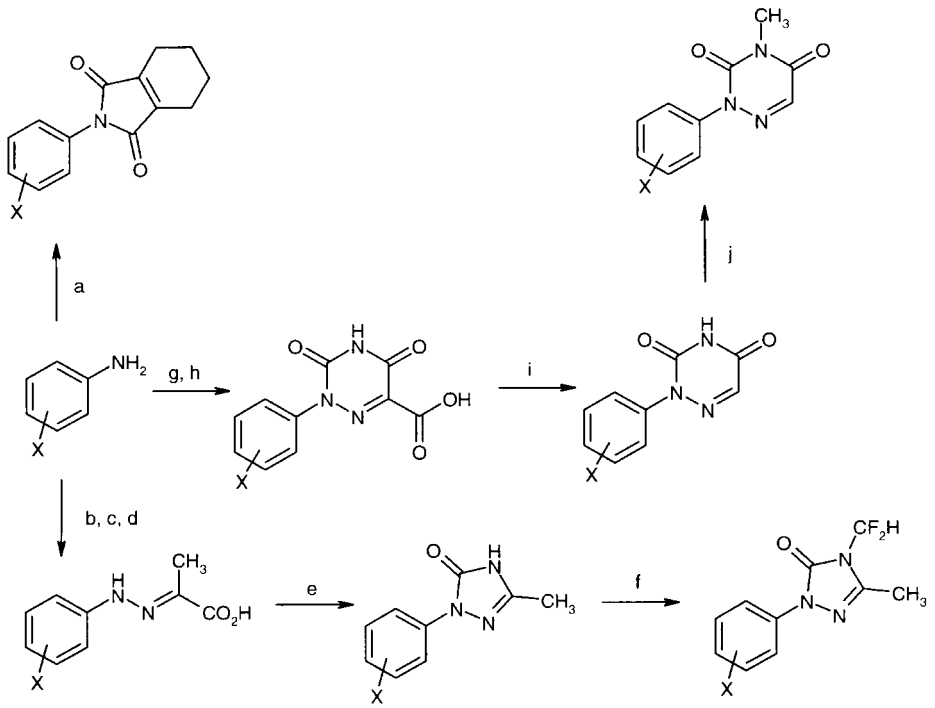

Figure 3. Synthesis of heterocycles **1**, **2**, and **3**. a. 3,4,5,6-tetrahydrophthalic anhydride, acetic acid, 100°, 120 min; b. $NaNO_2$, HCl, 0°, 15 min; c. $SnCl_2$, HCl, 0°, 30 min; d. CH_3COCO_2H, H_2O, 30 min; e. diphenylphosphoryl azide, toluene, TEA, 100°, 60 min; f. $CHClF_2$, DMF, K_2CO_3, 100°, 60 min; g. $CH_2(CONHCO_2Et)_2$, NaOAc, HCl, $NaNO_2$, H_2O; h. KOH, H_2O; i. $HSCH_2CO_2H$, 150°, 2 h; j. CH_3I, NaH, DMF, 60 min.

benzoxazinone herbicides **2**–**4** have been reported elsewhere.[2–4]

2.2 Biological evaluation

2.2.1 Hydroponic cucumber assay (hydrocuke)

The hydrocuke assay is a hydroponic assay using etiolated cucumber explants (*Cucumis sativus* L cv Wisconson), retaining the cotyledons, apical meristem, and upper portions of the stem. A pI_{50} value ($-\log$ M) for each test compound was calculated from the relative growth inhibition measured as fresh weight gain after treatment relative to that of untreated controls.[10]

2.2.2 Protox assay

The protox assay uses a unicellular microalga *Chlamydomonas renhardii* Dang y-1 mutant which is unable to synthesize chlorophyll in the dark. Algae are depleted of chlorophyll by growing in the dark for several generations; chlorophyll synthesis resumes when they are exposed to light. After treatment of the algae with the test compound and incubation

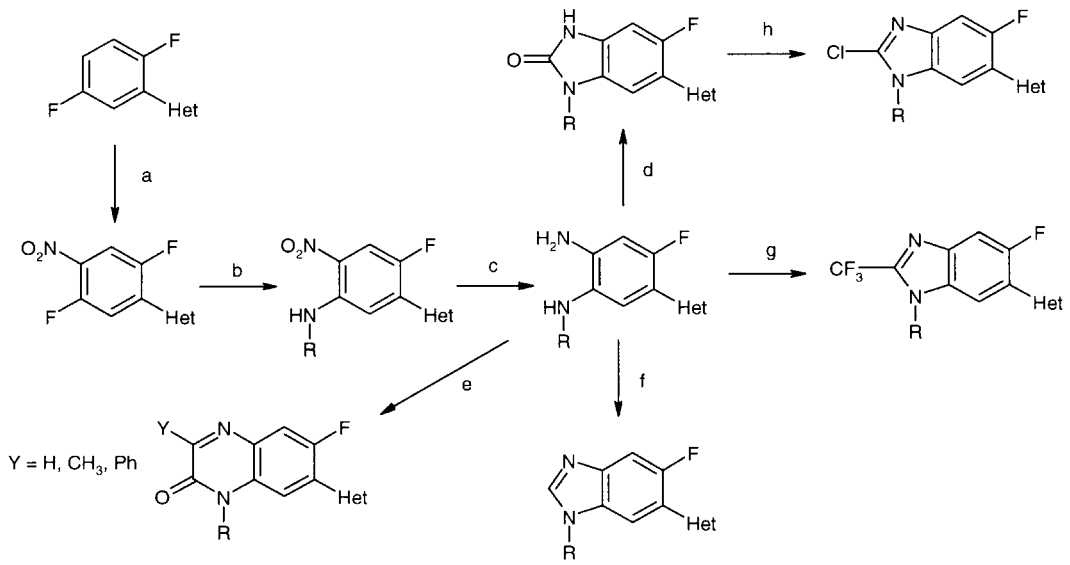

Figure 4. Synthesis of benzoxazinone replacements from 2,5-difluorophenyl heterocycles. a. H_2SO_4, HNO_3, 10°, 30 min; b. alkyl amine, THF, TEA, 100°, 30 min; c. Fe, acetic acid, H_2O, 80°, 60 min; d. carbonyldiimidazole, THF, 70°, 180 min; e. $YCOCO_2Et$; toluene, 100°, 90 min; f. $HC(OEt)_3$, dioxane, H_2SO_4, 80°, 60 min; g. CF_3CO_2H, 70°, 30 min; h. $POCl_3$, 70°, 3 h.

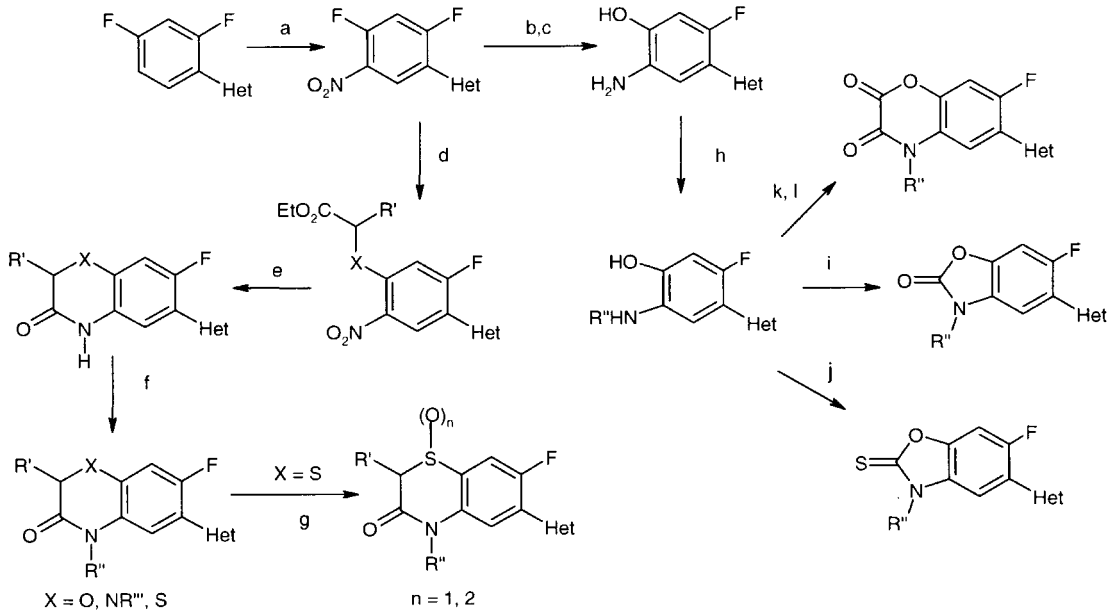

Figure 5. Synthesis of benzoxazinone replacements from 2,4-difluorophenyl heterocycles. a. H_2SO_4, HNO_3, 10°, 15 min; b. *N*-hydroxysuccinimide, NaH, DMF, 15 min; c. Fe, acetic acid, ethanol, H_2O, 10°, 15 min; d. X=O; HOR'$CHCO_2Et$, NaH, THF, 0°, 30 min; X=NR‴, HR‴NR'$CHCO_2Et$, TEA, dioxane, 100°, 180 min; X=S, HSR'$CHCO_2Et$, KOH, DMF, 80°, 15 min; e. Fe, acetic acid, H_2O, 80°, 30 min; f. R″X, NaH, DMF, 60 min; g. mCPBA, CH_2Cl_2, 60 min; h. R″X, K_2CO_3, CH_3CN, H_2O, 80°, 15 min; i. carbonyldiimidazole, THF, 10°, 60 min; j. thiophosgene, TEA, CH_2Cl_2, 30 min; k. (*N*-imidazolyl)$COCO_2Et$, THF, 10 min; l. amberlite IR-120, H_2O, 5 min.

under continuous illumination, the inhibition of protox is determined by measuring the accumulation of protoporphyrin IX ($-\log$ M, where M is the concentration required to cause a 50% increase) using a fluorescence microtitre plate reader.

2.3 QSAR and 3D graphics methods

2.3.1 Bicyclic molecular properties

The molecular properties for the bicyclic core (R = propyl) were calculated without the attached heterocycle. Indicator variables for the heterocycle (**3**) and *N*-alkyl group (**2**) were used in the final analysis. All calculations were done on a Silicon Graphics® workstation (Silicon Graphics, Inc) using Cerius^2® software (Molecular Simulations, Inc). The low-energy conformers for the bicyclic compounds were generated using Alchemy® 2000 or Sybyl® (Tripos Associates, Inc). The molecular properties were selected to cover energy properties (HOMO and LUMO), electronic properties (dipole moment, dipole direction, and superdelocalizability), spatial/steric properties (molecular volume, molecular mass, surface projections along the *xy*, *yz* and *xz* planes, and molecular length along the *x*, *y* and *z* coordinates), and thermodynamic properties (calculated log *P* and calculated molar refractivity). Analysis of the data was done using JMP® (SAS Institute) programs.

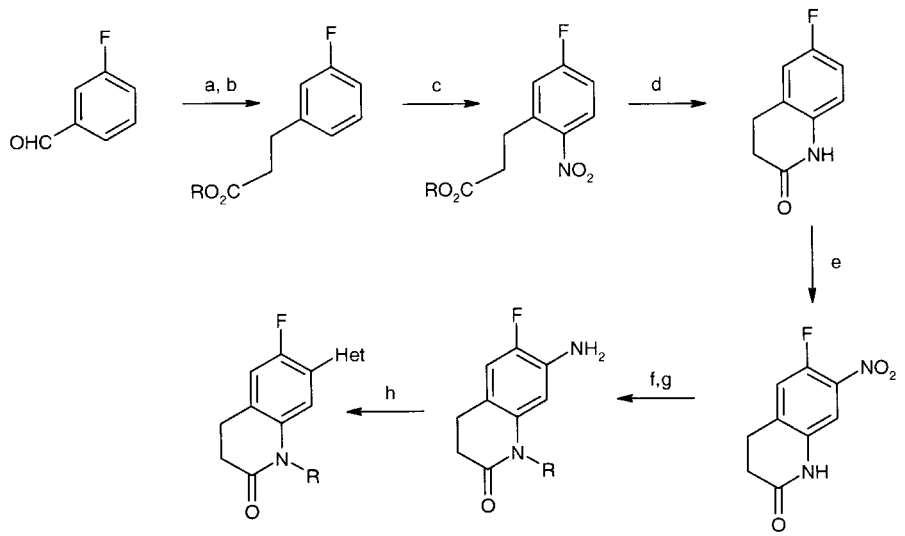

Figure 6. Synthesis of benzoxazinone replacements from 3-fluorobenzaldehyde. a. (carboethoxymethylene)triphenylphosphorane; CH_2Cl_2, 30 min; b. PtO_2, H_2, EtOH, 60 min; c. H_2SO_4, HNO_3, 10°, 30 min; d. PtO_2, H_2, EtOH, 60 min; e. H_2SO_4, HNO_3, 10°, 30 min; f. K_2CO_3, DMF, R″X, 70°, 30 min. g. Fe, acetic acid, H_2O, 50°, 90 min; h. See Fig 3.

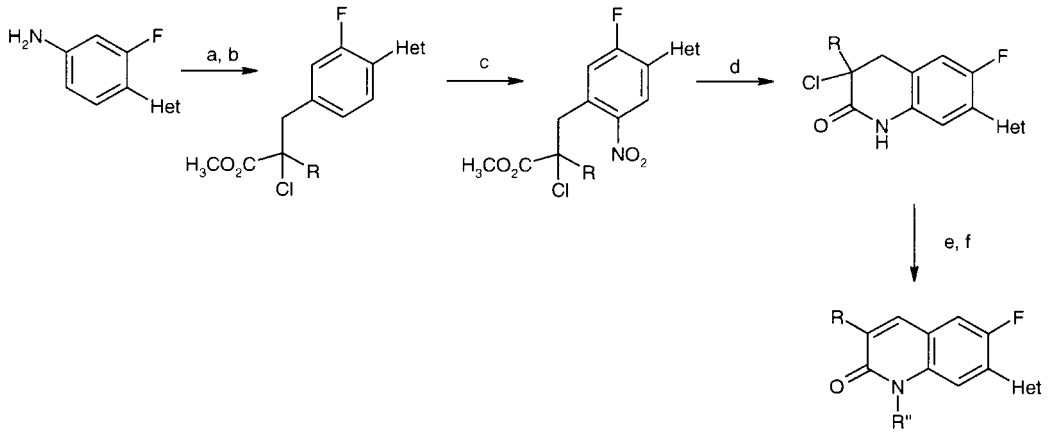

Figure 7. Synthesis of benzoxazinone replacements from 2-fluoro-4-aminophenyl heterocycles. a. HCl, acetone, $NaNO_2$, 10°, 30 min; b. CH_2=$CRCO_2R'$, CuCl, 0° to 25°, 60 min; c. H_2SO_4, HNO_3, 10°, 90 min; d. Fe, acetic acid, H_2O, 50°, 90 min; e. THF, TEA, 25°, 60 min; f. K_2CO_3, DMF, R″X, 70°, 30 min.

2.3.2 *3D Graphics calculations*

The molecular electrostatic potential energy maps and the HOMO and LUMO molecular orbitals were calculated using Spartan™ software (Wavefunction, Inc). The semi-empirical geometry optimization method was used with the Merck force field.

3 RESULTS

3.1 QSAR of the bicyclic protox inhibitors using molecular properties

We synthesized a number of 5- and 6-membered bicyclic ring replacements with the goal of developing structure–activity relationships. The ring systems clustered into three groups: highly active; moderately active; and weakly active (Fig 9) as determined using the hydrocuke and protox assays (Table 1). The most obvious features of the highly active cluster were the presence of an unsubstituted heteroatom at position 4 of the aryl ring, the presence of an amide C=O, and lack of bulky and/or electronegative appendages. Since we did not have the traditional fragment properties such as π, σ, or MR, etc, for many of these replacements in our QSAR database, we elected to develop structure–activity relationships using molecular properties.

There have been several recent reports which have correlated bulk, electronic and energy properties with protox activity for acyclic protox inhibitors.[11–15] Based in part on these reports, we selected 26 molecular descriptors, including energy properties (HOMO and LUMO), electronic properties (dipole moment, dipole direction and superdelocalizability), spatial/steric properties (molecular volume, molecular mass, surface projections along the *xy*, *yz*, and *xz* planes, and molecular length along the *x*, *y*, and *z* coordinates), and thermodynamic properties (calculated log *P* and calculated molar refractivity) to use in the analysis. We also included five indicator variables to factor out the differences due to the heterocycles and *N*-alkyl groups. All of the molecular properties were subjected to a stepwise regression analysis using the protox data. The best model (eqn (1)) included an energy term (HOMO), electrostatic terms (both the magnitude of the dipole and dipole direction), and a spatial term (surface area); all terms were significant at the 95% confidence level. This result is similar to the QSAR reported for the acyclic protox inhibitors

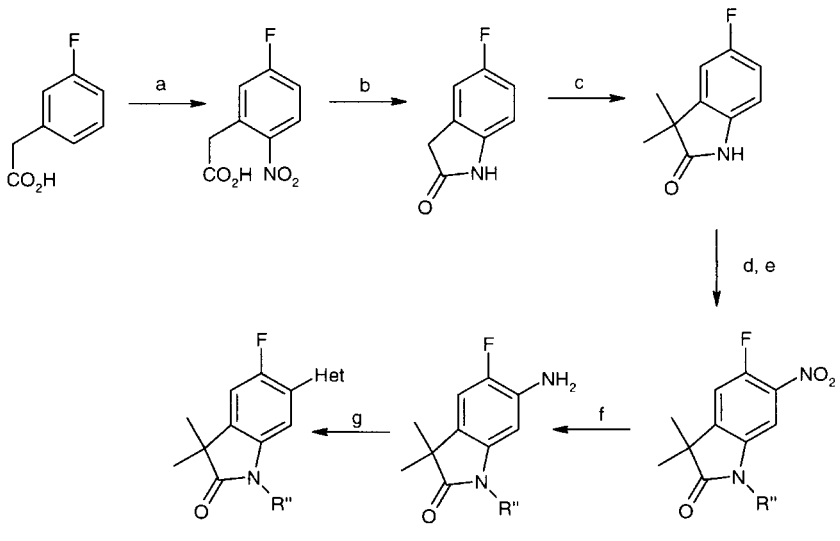

Figure 8. Synthesis of benzoxazinone replacements from 3-fluorophenylacetic acid. a. H_2SO_4, HNO_3, 25°, 3 h; b. PtO_2, AcOH, H_2, 1 h; c. CH_3I, DMF, NaH, 25°, 1 h; d. $CH_3CH_2CH_2I$, DMF, K_2CO_3, 25°, 3 h; e. H_2SO_4, HNO_3, 10°, 30 min; f. Fe, acetic acid, H_2O, 50°, 90 min; g. see Fig 3.

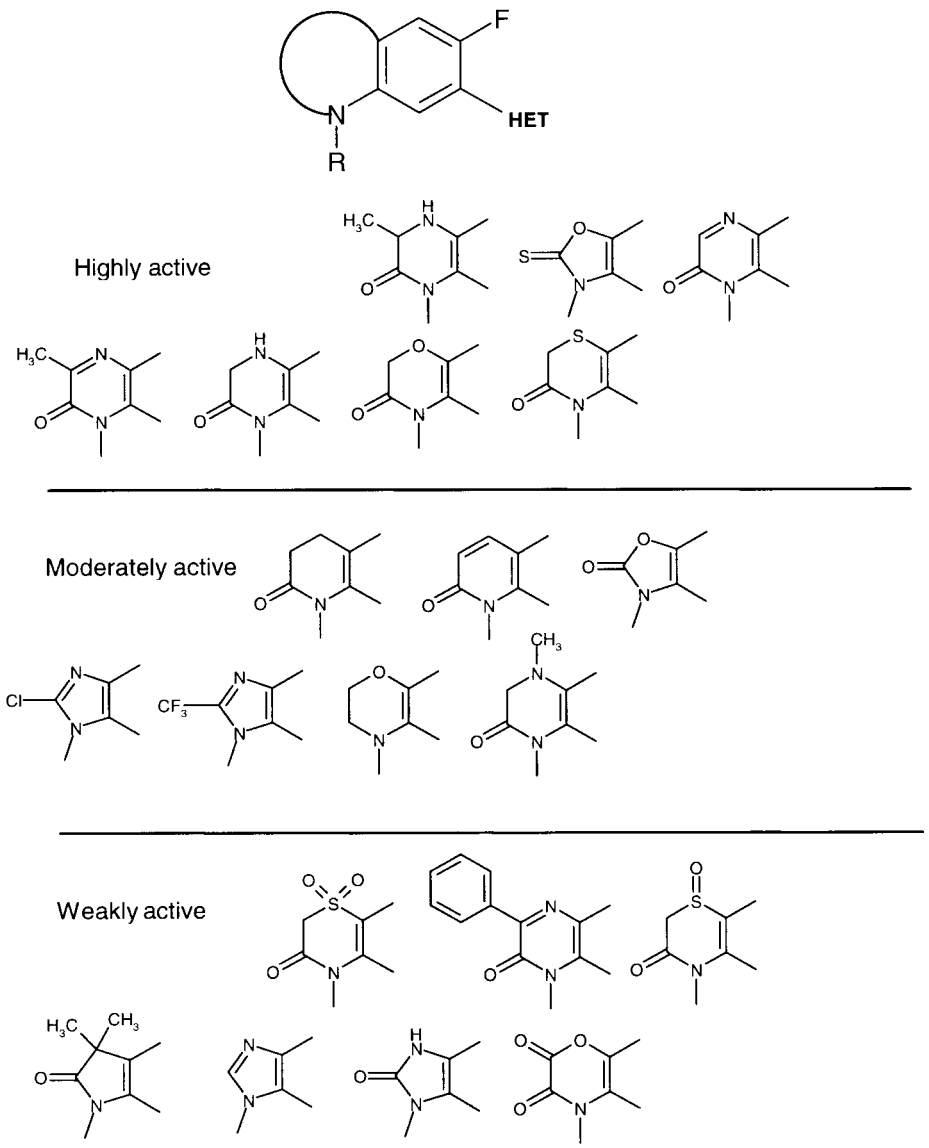

Figure 9. Relative herbicidal activity of the benzoxazinone replacements.

using molecular properties.[15] The significance of the log P and molecular volume terms in predicting hydrocuke activity from the protox activity (eqn (2)) is most likely due to the differential uptake of the test compounds between the two assays (Table 2).
Equation (1):

$$\text{Protox } pI_{50} = 1.63\ \text{HOMO} - 0.15\ \text{Dipole} + 0.39\ \text{DipoleX} - 0.20\ \text{Surface} + 31.1$$

$r^2 = 0.71$; $n = 24$; $F = 11.1$; HOMO ± 0.45, $t = 0.002$; Dipole ± 0.15, $t = 0.001$; DipoleX ± 0.12, $t = 0.005$; Surface ± 0.04, $t = 0.001$.
Equation (2):

$$\text{Hydrocuke } pI_{50} = 0.51\ \text{Protox} - 0.02\ \text{Volume} + 0.57 \log P + 5.10$$

$r^2 = 0.70$; $n = 21$; $F = 13.3$; Protox ± 0.11, $t = 0.001$; Volume ± 0.007, $t = 0.040$; log P ± 0.17, $t = 0.004$.

Since the QSAR for the acyclic and bicyclic protox inhibitors were so similar, we decided to examine 3D graphical models more closely. Comparisons of the HOMO and LUMO molecular orbital maps or the acyclic and bicyclic protox inhibitors (Plate 1) show that they have very similar energy properties. The molecular electrostatic potential energy maps (Plate 2) are also very similar, except for the added electropositive region (blue arrow) for the methylene bridge of the benzoxazinone. Both maps show an electronegative region (red arrow); the amide C=O of the benzoxazinone and the alkyl ether oxygen of the acyclic, which may be an H-bond acceptor interaction site within the protogen binding site.

Table 1. Intrinsic herbicidal activity for benzoxazinone replacements

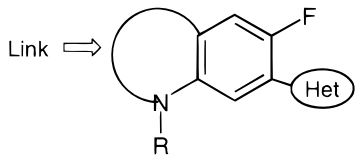

Link	*R*[a]	*Het*[b]	*Protox* pI_{50}	*Hydrocuke* pI_{50}
$C(CF_3)N$	1	3	6.6	6.4
$C(CF_3)N$	1	1	5.4	6.4
C(Cl)N	1	3	[c]	5.8
CH_2CH_2O	1	1	5.5	7.1
CHN	1	1	5.2	5.6
$COC(CH_3)_2$	1	1	3.5	6.1
$COC(CH_3)N$	1	3	7.7	7.1
$COCH(CH_3)NH$	2	3	7.6	[c]
$COCH(CH_3)NH$	2	2	[c]	7.8
$COC(CH_3)CH$	2	1	7	7.8
$COCH_2CH_2$	1	1	6.4	6.8
$COCH_2CH_2$	1	2	7.2	[c]
$COCH_2NH$	1	3	[c]	7.4
$COCH_2NH$	2	3	7.6	[c]
$COCH_2NH$	2	2	[c]	7.7
$COCH_2O$	1	3	7.6	7.3
$COCH_2O$	1	1	7.1	8.2
$COCH_2O$	2	1	[c]	8.8
$COCH_2O$	1	2	7.9	7.7
$COCH_2O$	2	2	[c]	8
$COCH_2S$	1	1	[c]	7.2
$COCH_2SO$	1	1	4.3	4.3
$COCH_2SO_2$	1	1	[c]	5.4
COCH=CH	1	1	6	7.8
COCH=CH	1	2	[c]	8
COCH=N	1	3	7.4	7.2
COCH=N	2	2	[c]	7.8
COCOO	1	3	5.5	6.1
COCOO	2	2	[c]	7.8
COC(Ph)N	1	3	5.9	5.6
CONH	1	3	[c]	4.5
COO	1	3	7.1	6.8
COO	1	1	6.5	7.6
COO	1	2	7.7	7.5
CSO	1	3	7.6	7.1
CSO	2	3	[c]	7.7
CSO	2	2	[c]	8.1

[a] 1 = propyl; 2 = propargyl.
[b] See Fig 1 for heterocycles.
[c] Not determined.

4 CONCLUSIONS

The intrinsic herbicidal activity for the bicyclic protox inhibitors is influenced by molecular properties, including the energy of the HOMO, the magnitude and direction of the dipole moment and by steric properties. The most active compounds have an unsubstituted heteroatom at position 4 of the aryl ring, the presence of an amide C=O, and lack bulky and/or electronegative appendages. That the molecular properties of the acyclic and bicyclic protox inhibitors are similar suggest they may be interacting with the same protox binding site.

ACKNOWLEDGEMENTS

We thank M. Joan Plummer and her team for running the hydrocuke and protox assays and Dr Litai Zhang for help with calculating the molecular descriptors.

REFERENCES

1 Nagano E, Haga T, Sato R and Morita K, Eur Pat Appl EP 170191 (1985) [CAN 105:563501].
2 Chang JH and Lyga JW, Tetrazolinone herbicides. US Patent 4,734,124 (1988).
3 Chang JH and Lyga JW, Triazinedione herbicides. US Patent 4,755,217 (1988).
4 Chang JH and Lyga JW, Triazolin-5-one herbicides. US Patent 4,761,174 (1988).
5 Lyga JW, Halling BP, Witkowski DA, Patera RM, Seeley JA, Plummer MJ and Hotzman FW, Synthesis, herbicidal activity, and action mechanism of 2-aryl-1,2,4-triazine-3,5-diones, in *Synthesis and Chemistry of Agrochemicals II*, ed by Baker DR, Fenyes JG and Moberg WK, ACS Symposium Series 443, Am Chem Soc, Washington, DC. pp 170–181 (1991).
6 Lyga JW, Patera RM, Theodoridis G, Halling BP, Hotzman FW and Plummer MJ, Synthesis and quantitative structure–activity relationships of herbicidal *N*-(2-fluoro-5-methoxyphenyl)-3,4,5,6-tetrahydrophthalimides, *J Agric Food Chem* **39**:1667–1673 (1991).
7 Theodoridis G, Baum JS, Hotzman FW, Manfredi MC, Maravetz LL, Lyga JW, Tymonko JM, Wilson KR, Poss KM and Wyle MJ, Synthesis and herbicidal properties of aryltriazolinones, in *Synthesis and Chemistry of Agrochemicals III*, ed by Baker DR, Fenyes JG and Steffens JJ, ACS Symposium Series 504, Am Chem Soc Washington, DC. pp 134–146 (1992).
8 Theodoridis G, Structure–activity relationships of herbicidal aryltriazolinones. *Pestic Sci* **50**:283–290 (1997).
9 Theodoridis G, Baum JS, Chang JH, Crawford SD, Hotzman FW, Lyga JW, Maravetz LL, Suarez DP and Hatterman-Valenti H, Synthesis and Herbicidal Activity of Fuzed Benzoheterocyclic Ring Systems, in *Synthesis and Chemistry of Agrochemicals V*, ed by Baker DR and Fenyes JG, ACS Symposium Series 686, Am Chem Soc Washington, DC. Ch 8 (1998).
10 Lyga JW, Patera RM, Theodoridis G, Halling BP, Hotzman FW and Plummer MJ, Synthesis and quantitative structure–activity relationships of herbicidal *N*-(2-fluoro-5-methoxyphenyl)-3,4,5,6-tetrahydrophthalimides. *J Agric Food Chem* **39**:1667–1673 (1991).
11 Nandihalli UB, Duke MV and Duke SO, Quantitative structure–activity relationships of protoporphyrinogen oxidase-inhibiting diphenyl ether herbicides, *Pestic Biochem Physiol* **43**:193–211 (1992).
12 Nandihalli UB, Duke MV and Duke SO, Relationships between molecular properties and biological activities of *o*-phenyl pyrrolidino- and piperidinocarbamate herbicides, *J Agric Food Chem* **40**:1993–2000 (1992).

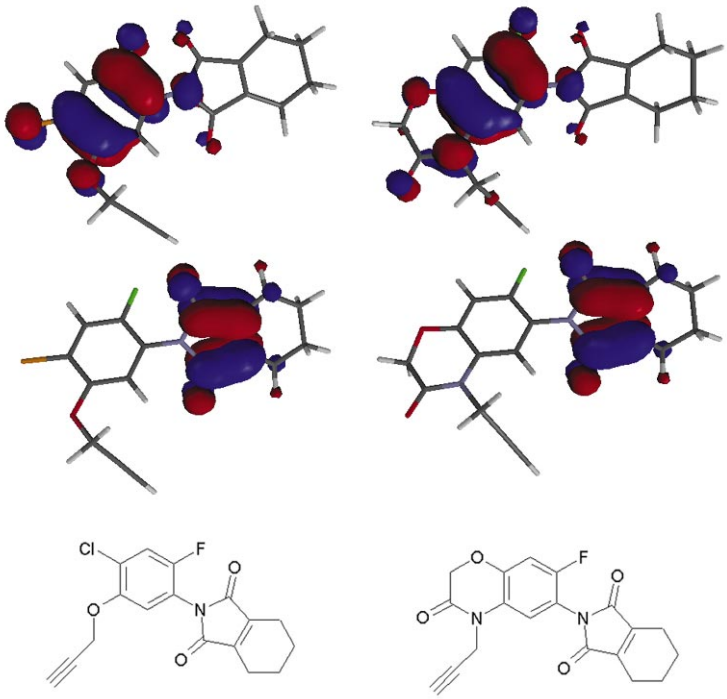

Plate 1. Comparisons of the HOMO (top) and LUMO (bottom) molecular orbital maps for the acyclic (left) and bicyclic (right) protox inhibitors.

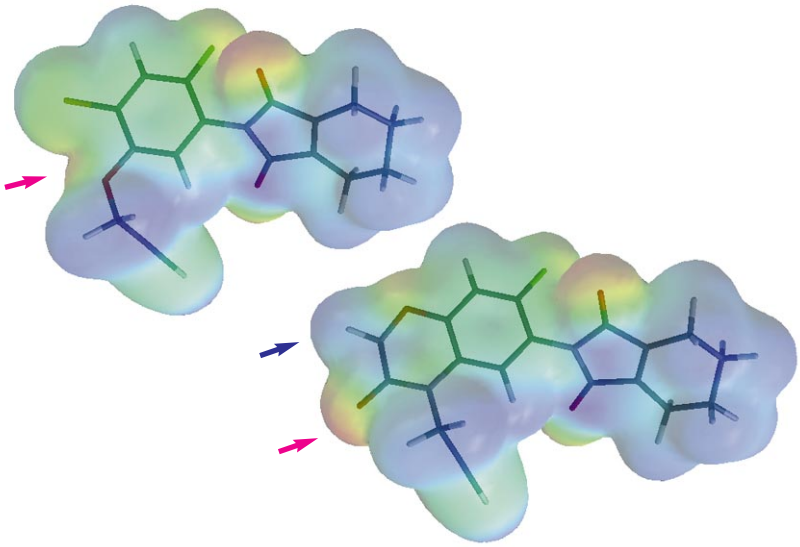

Plate 2. The molecular electrostatic potential energy maps for the acyclic (top left) and bicyclic (bottom right) protox inhibitors (see Plate 1). The blue arrow indicates an electropositive region and the red arrow indicates an electronegative region.

Link	*HOMO*[a]	*Dipole*[b]	*Dipole x*[c]	*Surface*[d]	*Volume*[e]	*Log P*[f]
$C(CF_3)N$	−11.05	2.52	−0.76	26.3	192.38	2.85
C(Cl)N	−11.35	3.15	−2.03	24.34	178.13	1.91
CH_2CH_2O	−10.17	2.91	−2.51	29.61	183.13	3.56
CHN	−10.6	3.53	−3.3	21.1	161.27	1.91
$COC(CH_3)_2$	−10.7	1.08	0.3	40.7	211.62	4.55
$COC(CH_3)N$	−10.28	1.03	0.46	32.18	198.32	3.16
$COCH(CH_3)NH$	−10.18	0.39	−0.21	34.29	192.13	1.65
$COC(CH_3)CH$	−10.63	0.68	0.65	31.73	191.94	3.28
$COCH_2CH_2$	−10.64	0.66	0.32	33.47	192.29	4.06
$COCH_2NH$	−10.13	0.21	0.04	27.29	187.18	2.57
$COCH_2O$	−10.64	1.43	0.94	31.5	184.3	3.45
$COCH_2S$	−10.88	1.44	0.95	37.81	193.57	2.8
$COCH_2SO$	−8.96	6.73	−5.81	30.27	196.97	1.45
$COCH_2SO_2$	−9.07	6.59	4.82	32.51	203.92	1.45
COCH=CH	−10.5	1.24	−0.23	32.14	186.68	3.81
COCH=N	−10.58	1.54	0.3	26.39	181.45	2.46
COCOO	−10.74	3.33	1.08	27.69	186.96	2.33
COC(Ph)N	−10.18	1.15	0.59	37.08	252.57	4.03
CONH	−10.42	1.34	0.31	22.92	172.12	2.04
COO	−10.82	2.82	−0.2	22.58	168.98	2.92
CSO	−9.89	4.56	1.61	24.61	179.29	2.48

[a] HOMO – highest occupied molecular orbital.
[b] DIPOLE – magnitude of the dipole moment.
[c] DIPOLE X – *x* component of the dipole moment.
[d] SURFACE – surface area projected on an *xy* plane.
[e] VOLUME – molecular volume.
[f] Log *P* – calculated octanol-water partition coefficient.

Table 2. Molecular properties for benzoxazinone replacements

13 Nandihalli UB and Duke SO, Structure–activity relationships of protoporphyrinogen oxidase inhibiting herbicides, in *Porphyric Pesticides, Chemistry, Toxicology, and Pharmaceutical Applications*, ed by Duke SO and Rebeiz CA, ACS Symposium Series 559, Am Chem soc, Washington, DC, pp 133–146 (1994).
14 Dayan FE, Duke SO, Reddy KN, Hamper BC and Leschinsky KL, Effects of isoxazole herbicides on protoporphyrinogen oxidase and porphyrin physiology, *J Agric Food Chem* **45**:967–975 (1997).
15 Reddy KN, Nandihalli UB, Lee HJ, Duke MV and Duke SO, in *Computer-Aided Molecular Design. Applications in Agrochemicals, Materials, and Pharmaceuticals*, ed by Reynolds QA, Holloway MK and Cox HK, ACS Symposium Series 589, Am Chem Soc Washington, DC. Ch 15 (1995).